All-Metal Domestic Induction Heating Using Single-Frequency Double-Layer Coils

Wei Han, K. T. Chau, *Fellow, IEEE*, Chaoqiang Jiang, and Wei Liu

Department of Electrical and Electronic Engineering, University of Hong Kong, Hong Kong

This paper proposes and implements a single-frequency double-layer coil system for all-metal domestic induction heating. Traditional induction heating has been developed to effectively heat a ferromagnetic pan, but is incapable of heating a non-ferromagnetic pan as it will cause high current stress at the power source. Inevitably, this limitation has hampered the popularization of existing induction heating. The proposed system consists of double-layer concentric coils with their compensated capacitors connected in series. The key is to employ the magnetic resonant coupling mechanism to strengthen the magnetic coupling and hence to enhance the power transfer between the coil and the pan. Differing from using a higher frequency to separately heat the non-ferromagnetic pan, the proposed system can employ a single frequency to operate at the high-voltage low-current and low-voltage high-current modes to effectively heat the ferromagnetic and non-ferromagnetic pans, respectively. Moreover, the required high current can be shifted from the primary coil to the resonant coil, hence significantly reducing the current stress at the power source. Both simulation and experimental results are given to validate the feasibility of the proposed induction heating.

Index Terms— **Double-layer coils, ferromagnetic pan, induction heating, magnetic resonant coupling (MRC), non-ferromagnetic pan.**

I. Introduction

GIVEN high efficiency, high controllability, and inherent safety, induction heating has been rapidly developed in the past few decades. For conventional induction heating, an ac power source is employed to energize the heating coil to generate a time-varying magnetic field, which accordingly induces eddy current and magnetic hysteresis in the ferromagnetic pan to produce the heating effect [1]. However, those pans made of non-ferromagnetic materials, such as stainless steel, aluminum, and copper, cannot be properly heated, which inevitably limits its functionality and convenience as compared with traditional open-fire heating.

Some researchers have dedicated to developing induction heating for both ferromagnetic and non-ferromagnetic pans, dubbed all-metal induction heating. For instance, superconducting windings were employed to produce strong magnetic field for induction heating of a cylindrical non-ferromagnetic workpiece [2]. However, such arrangement was not suitable for domestic induction heating. On the other hand, the operating frequency was doubled by using two inverters working in a time-sharing mode to achieve all-metal induction heating [3]. Meanwhile, by using the first-harmonic operation mode with the frequency of 22.5 kHz to heat the ferromagnetic pan and the third-harmonic operation mode with the frequency of 67 kHz to heat the non-ferromagnetic pan, the selective operating frequency technique was developed for all-metal domestic induction heating [4]. In addition, by changing the operating frequency and input voltage to accommodate pans with various materials, an inverter possessing load-adaptive modulation was developed for all-metal induction heating applications [5]. Unavoidably, the use of frequency selection involves additional switching losses, which will deteriorate the heating efficiency and worsen the electromagnetic interference.

In recent years, the magnetic resonant coupling (MRC) mechanism has been widely developed for wireless power transfer, such as for electric vehicle charging [6], wireless motors [7], wireless lighting [8], and flexible heating [9]. Recently, by further employing the MRC mechanism, the homogeneity of induction heating has been improved significantly [10].

In this paper, the MRC mechanism is further extended to help heat up non-ferromagnetic materials. Hence, a new all-metal domestic induction heating system is proposed and implemented. In essence, the high-voltage low-current mode of operation is utilized to heat the ferromagnetic pan, and the low-voltage high-current mode of operation is to heat the non-ferromagnetic pan. Consequently, the proposed all-metal induction heating can attain the advantages of single operating frequency, simplicity, and low electromagnetic interference.

Section II will adopt the circuit-model-based method to assess the influence of metallic materials on induction heating. Section III will carry out the computational simulation of the corresponding electromagnetic and thermal fields. Finally, in Section IV, an experimental prototype will be constructed and tested so as to further verify the feasibility of the proposed induction heating.

II. Proposed Induction Heating

As shown in Fig. 1, the proposed induction heating mainly consists of the lower primary coil and upper resonant coil with their compensated capacitors connected in series. A 30 kHz ac power supply serves to energize the lower primary coil, which in turn induces eddy currents in the pan; while the upper resonant coil is indirectly excited by the lower primary coil which also induces eddy currents in the pan too. Meanwhile,

Manuscript received March 7, 2018; revised May 10, 2018; accepted June 6, 2018. Corresponding author: K. T. Chau (e-mail: ktchau@eee.hku.hk).

Color versions of one or more of the figures in this paper are available online at http://ieeexplore.ieee.org.

Digital Object Identifier 10.1109/TMAG.2018.2846548

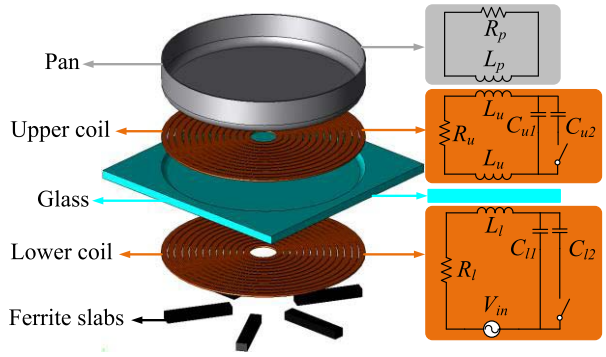

Fig. 1. Structure of proposed induction heating.

TABLE I
KEY PARAMETERS OF PROPOSED INDUCTION HEATING

Item	Value
Lower coil number of turns	20
Lower coil inductance (ferromagnetic)	5.03×10^{-5} H
Lower coil inductance (non-ferromagnetic)	1.47×10^{-5} H
Lower coil internal resistance	0.21 Ω
Lower coil capacitance (ferromagnetic)	8.04×10^{-7} F
Lower coil capacitance (non-ferromagnetic)	1.93×10^{-6} F
Upper coil number of turns	20
Upper coil inductance (ferromagnetic)	7.12×10^{-5} H
Upper coil inductance (non-ferromagnetic)	4.07×10^{-5} H
Upper coil internal resistance	0.20 Ω
Upper coil capacitance (ferromagnetic)	4.29×10^{-7} F
Upper coil capacitance (non-ferromagnetic)	6.92×10^{-7} F
Glass thickness	5 mm
Ferrite bar size (length×width×height)	8.5×1.5×0.5 cm
Lower and upper coil inner/outer diameter	4/18 cm
Pan diameter	18 cm
Input power	450 W
Resonant frequency	30 kHz

ferrite slabs have been placed beneath the coils to improve the performance of the whole induction heating system. Across the compensated capacitor of each coil, a switched-capacitor branch consisting of one power switch and one capacitor is added to ensure the MRC under the single frequency when heating ferromagnetic and non-ferromagnetic pans. Specifically, when heating the ferromagnetic pan, the power switches are opened so that only C_{l1} and C_{u1} are connected in series with the lower and upper coils, respectively; when heating the non-ferromagnetic pan, the power switches are closed so that $(C_{l1}+C_{l2})$ and $(C_{u1}+C_{u2})$ are connected in series with the lower and upper coils, respectively. And all relevant parameters of Fig. 1 are listed in Table I.

In order to reveal the relationship between output power and material of the pan, the equivalent circuits of the proposed system are shown in Fig. 2, where L_l, L_u, and L_p are the self-inductances of the lower primary coil, upper resonant coil, and pan, respectively; R_l, R_u, and R_p are their internal resistances, respectively; $M_{\rm lu}$ and $M_{\rm up}$ are the mutual inductances through direct magnetic coupling; $M_{\rm lp}$ is the mutual inductance through cross magnetic coupling; and C_l and C_u are equivalent compensated capacitors in the lower and upper coils, respectively.

By referring the pan to the lower and upper coils, the equivalent circuit in Fig. 2(a) can be depicted as Fig. 2(b). Based on [9], the corresponding referred impedances $Z_{\rm lp}$ and

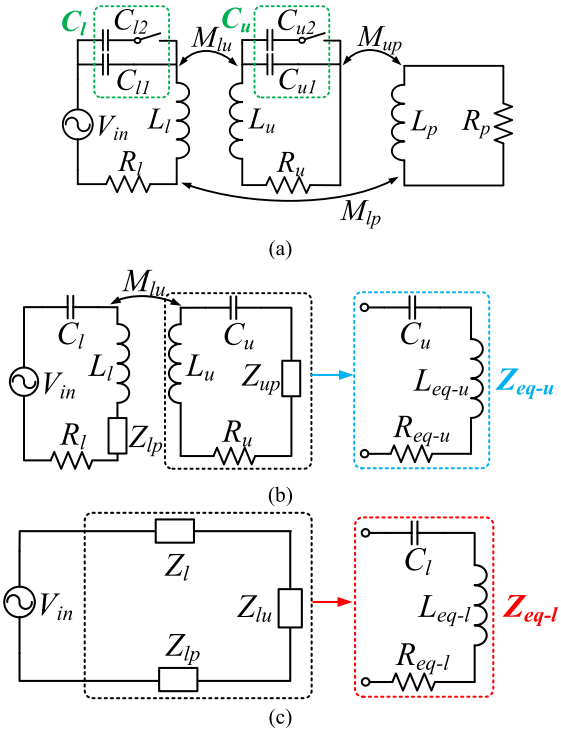

Fig. 2. Equivalent circuits. (a) Without referral. (b) Referred to lower and upper coils. (c) Referred to lower coil.

$Z_{\rm up}$ are given by

$$Z_{\rm lp}=\frac{(\omega M_{\rm lp})^2}{j\omega L_p+R_p} \tag{1}$$

$$Z_{\rm up}=\frac{(\omega M_{\rm up})^2}{j\omega L_p+R_p}. \tag{2}$$

Thus, the upper coil equivalent impedance can be expressed by

$$Z_{{\rm eq}-u}=\frac{1}{j\omega C_u}+j\omega L_u+R_u+\frac{(\omega M_{\rm up})^2}{j\omega L_p+R_p}. \tag{3}$$

Hence, the equivalent impedance, inductance, and resistance of the upper coil are written as

$$Z_{{\rm eq}-u}=\frac{1}{j\omega C_u}+j\omega L_{{\rm eq}-u}+R_{{\rm eq}-u} \tag{4}$$

$$L_{{\rm eq}-u}=L_u-AM_{\rm up}^2L_p \tag{5}$$

$$R_{{\rm eq}-u}=R_u+AM_{\rm up}^2R_p \tag{6}$$

where

$$A=\frac{\omega^2}{R_p^2+(\omega L)^2}. \tag{7}$$

Accordingly, the required capacitance in the upper coil can be calculated to fully compensate the equivalent inductance of the upper coil

$$C_u=\frac{1}{\omega^2L_{{\rm eq}-u}}. \tag{8}$$

According to (4) and (8), the inductance of the upper coil can be fully compensated by the capacitor at the resonant frequency so that the equivalent impedance of upper coil

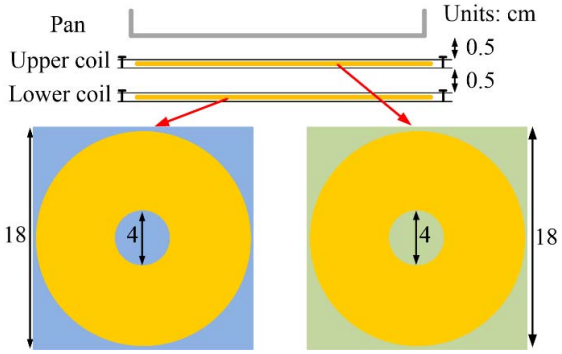

Fig. 3. Geometry of proposed induction heating.

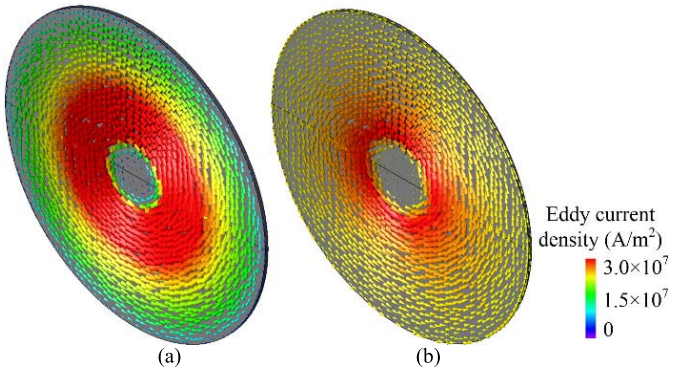

Fig. 4. Eddy current density distributions. (a) Ferromagnetic pan. (b) Non-ferromagnetic pan.

$Z_{\text{eq}-u}$ becomes a pure resistance $R_{\text{eq}-u}$. And by further referring the upper coil and pan to the lower coil as shown in Fig. 2(c), the equivalent input impedance can be obtained

$$\begin{cases} Z_l = j\omega L_l + 1/j\omega C_l + R_l \\ Z_{\text{lu}} = \dfrac{(\omega M_{\text{lu}})^2}{R_{\text{eq}-u}} \\ Z_{\text{eq}-l} = Z_l + Z_{\text{lp}} + Z_{\text{lu}}. \end{cases} \tag{9}$$

Hence, the equivalent impedance, inductance, and resistance of the lower coil are written as

$$Z_{\text{eq}-l} = \frac{1}{j\omega C_l} + j\omega L_{\text{eq}-l} + R_{\text{eq}-l} \tag{10}$$

$$L_{\text{eq}-l} = L_l - AM_{\text{lp}}^2 L_p \tag{11}$$

$$R_{\text{eq}-l} = R_l + AM_{\text{lp}}^2 R_p + \frac{(\omega M_{lu})^2}{R_{\text{eq}-u}}. \tag{12}$$

Accordingly, the required capacitance in the lower coil can be calculated to fully compensate the equivalent inductance of the lower coil

$$C_l = \frac{1}{\omega^2 L_{\text{eq}-l}}. \tag{13}$$

Therefore, when the applied frequency is equal to the resonant frequency, the resultant impedances of these double-layer coils become

$$\begin{cases} Z_{\text{eq}-u} = R_{\text{eq}-u} \\ Z_{\text{eq}-l} = R_{\text{eq}-l}. \end{cases} \tag{14}$$

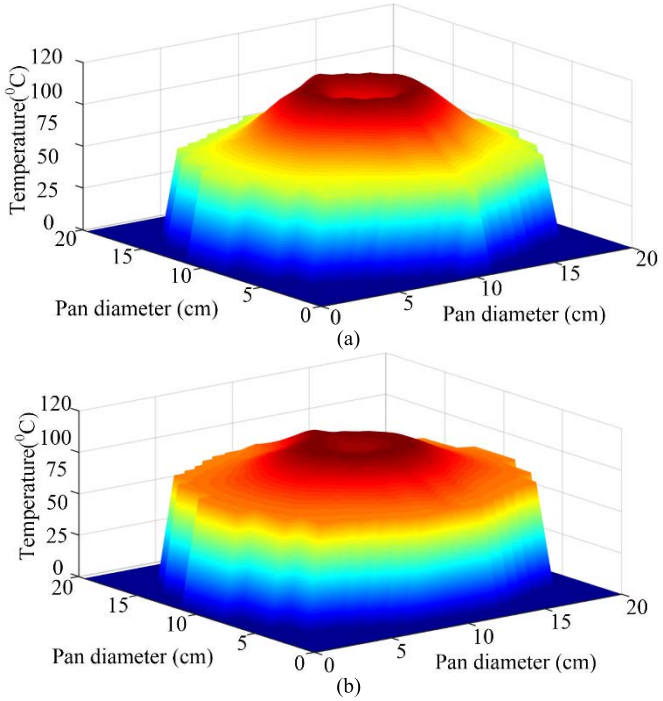

Fig. 5. Temperature distributions. (a) Ferromagnetic pan. (b) Non-ferromagnetic pan.

In addition, the internal resistance of upper coil R_u and lower coil R_l is the same and equal to R_0 because both coils utilize the same material and have the same number of turns. And according to [11], the resistance of the pan can be determined by the skin effect of eddy current. Thus, their resistances can be expressed as

$$\begin{cases} R_l = R_u = R_0 \\ R_p = \dfrac{\rho}{\delta} = 0.2\pi \times 10^{-3}\sqrt{\rho \mu_r f} \end{cases} \tag{15}$$

where δ is the skin depth and μ_r and ρ are the relative magnetic permeability and electrical resistivity of the material, respectively. Hence, the currents in the lower coil, upper coil, and the pan can be calculated based on Fig. 2 as well as (4), (9), and (14), which are given by

$$\begin{cases} I_l = \dfrac{V_{\text{in}}}{R_{\text{eq}-l}} \\ I_u = \dfrac{-j\omega M_{\text{lu}} V_{\text{in}}}{R_{\text{eq}-u} R_{\text{eq}-l}} \\ I_p = \dfrac{j\omega(M_{\text{lp}} I_l + M_{\text{up}} I_u)}{j\omega L_p + R_p}. \end{cases} \tag{16}$$

Based on (16), the actual output power dissipated in the pan is given by

$$P_{\text{out}} = \text{Re}(I_p^2 R_p) = \frac{1}{R_p}\left(\frac{\omega V_{\text{in}}}{R_p R_{\text{eq}-l} R_{\text{eq}-u}}\right)^2 \times [(M_{\text{lu}} M_{\text{up}})^2 + (\omega M_{\text{lp}} R_{\text{eq}-u})^2]. \tag{17}$$

Consequently, according to (17), the equivalent resistance of the pan R_p is relatively high when heating the ferromagnetic pan; the high-voltage (high V_{in}) low-current mode of operation

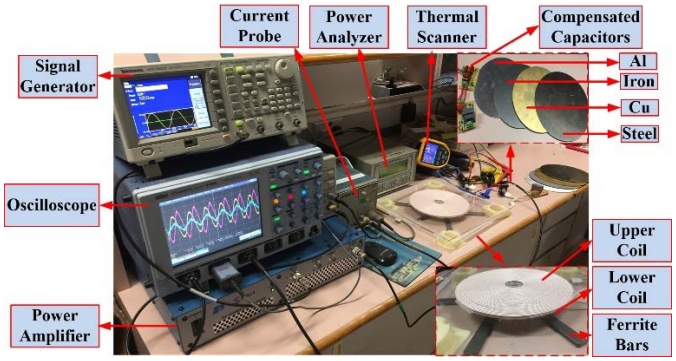

Fig. 6. Experimental prototype and testing setup.

is adopted to provide the desired output power. On the contrary, equivalent resistance R_p is relatively low when heating the non-ferromagnetic pan so that the low-voltage (low V_{in}) high-current model of operation is utilized to provide the same output power. Meanwhile, since the equivalent resistance of the lower coil as given by (12) is higher than that of the upper coil as given by (6), the required current is shifted from the lower coil to the upper coil so that the current stress at the power source can be significantly reduced when heating the non-ferromagnetic pan. In essence, both the lower and upper coils transmit power to the pan and the upper coil plays a major role because of its stronger magnetic coupling.

III. Computational Simulation

In order to illustrate the effectiveness of the proposed system, the finite-element method-based software package JMAG is employed to analyze the corresponding magnetic and thermal fields. The key parameters and geometry of the proposed induction heating system are shown in Table I and Fig. 3, respectively. The double-layer coils are of the same size: the outer diameter is 18 cm and the inner diameter is 4 cm.

As the induction heating effect is essentially due to the eddy current loss in the pan, the eddy current density at the bottom of the pan is simulated. The corresponding distributions in the ferromagnetic and non-ferromagnetic pans are shown in Fig. 4. It shows that the eddy current density in the ferromagnetic pan concentrates at the inner ring area and decreases rapidly at the outer area of the pan. In contrast, the eddy current density in the non-ferromagnetic pan has a smaller ring area and decreases gradually at outer area of the pan.

Consequently, the Joule loss density can be generated from the eddy current density. Hence, the temperature distributions in the ferromagnetic and non-ferromagnetic pans are calculated as shown in Fig. 5, in which each pan has been heated up for 120 s. For the ferromagnetic pan, due to its relatively high resistivity and relatively low thermal conductivity, the temperature distribution is more concentrated at the inner ring area. On the other hand, the non-ferromagnetic pan possesses relatively low resistivity and relatively high thermal conductivity so that its temperature distribution is more uniform. While there are variations in homogeneity, both the ferromagnetic and non-ferromagnetic pans can be heated properly to the desired temperature level.

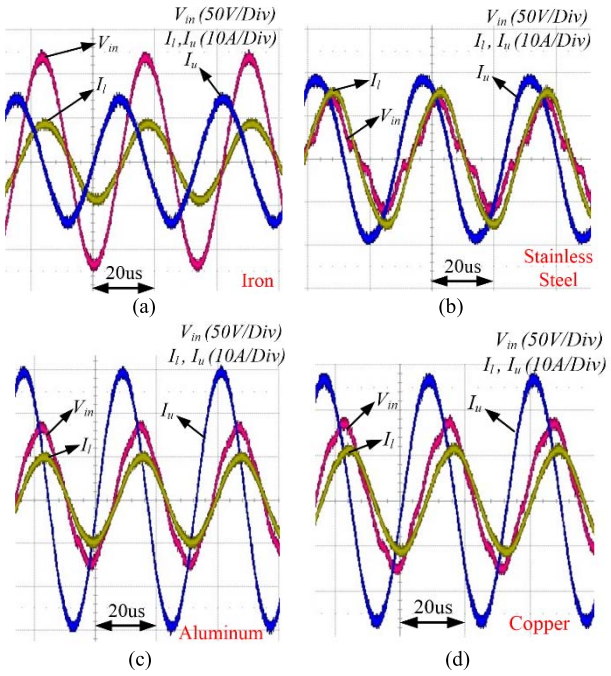

Fig. 7. Measured current and voltage waveforms. (a) Iron pan. (b) Stainless steel pan. (c) Aluminum pan. (d) Copper pan.

IV. Experimental Verification

An experimental prototype is constructed and its testing setup is established as shown in Fig. 6, in which the thermal image is captured by a non-contact thermal scanner (Fluke TiS40) and the ac power source is supplied by a power amplifier (E&I 1000S04). The input power is 450 W, which is measured by a power analyzer (PM300). Both the lower and upper coils are made of Litz wires to reduce the coil losses. The ferromagnetic pan is made of iron, whereas various non-ferromagnetic pans including the stainless steel, aluminum, and copper pans are adopted so as to fully verify the feasibility of the proposed all-metal induction heating. To facilitate accurate temperature measurement, the pan is purposely dry and empty. And the 30 kHz operating frequency is applied with the consideration of single operating frequency, simplicity, and low electromagnetic interference.

The measured waveforms of V_{in}, I_l, and I_u when heating ferromagnetic and non-ferromagnetic pans are shown in Fig. 7. For heating the ferromagnetic (iron) pan which has relatively high resistivity and high magnetic permeability, the high-voltage low-current mode of operation is adopted to provide the desired output power as depicted in Fig. 7(a), where the maximum values of V_{in}, I_l, and I_u are 120 V, 7.5 A, and 14 A, respectively. For heating the non-ferromagnetic pans, the low-voltage high-current mode of operation is adopted, where the maximum values of V_{in}, I_l, and I_u are 71 V, 12.5 A, and 19 A for the stainless steel pan, 82 V, 10.7 A, and 29 A for the aluminum pan, and 83 V, 11.1 A, and 27 A for the copper pan, respectively. The corresponding waveforms are depicted in Fig. 7 (b)–(d), respectively. It can be observed that the required high current is shifted from the lower coil to the upper coil, hence significantly reducing the current stress at the power source. Besides, in order to obtain the same

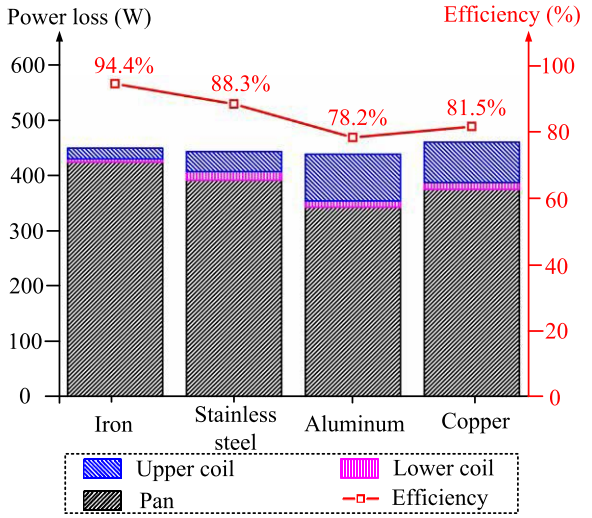

Fig. 8. Power loss and efficiency analyses of the rated power.

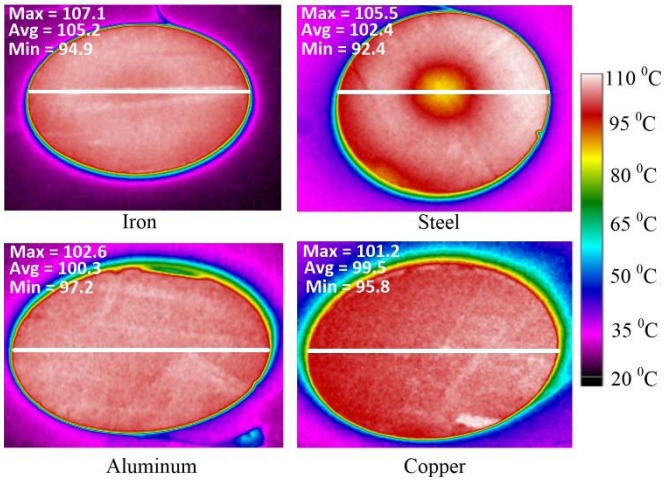

Fig. 9. Thermal images of various metallic pans.

desired power, the high-voltage low-current mode and low-voltage high-current mode are utilized to heat ferromagnetic and non-ferromagnetic pans as shown in Fig. 7, respectively. Thus, the experimental results can well agree with theoretical results in Section II.

Based on Fig. 7, the power loss and efficiency analyses when adopting ferromagnetic and non-ferromagnetic materials are shown in Fig. 8. When heating the iron, stainless steel, aluminum, and copper workpieces, the input (output) powers are 450 (424.8 W), 443.8 (392 W), 438.7 (343.2 W), and 460.7 W (375.4 W), respectively, so that the efficiencies are 94.4%, 88.3%, 78.2%, and 81.5%, respectively. Thus, the proposed single-frequency double-layer coils induction heating system can achieve higher efficiency for heating non-ferromagnetic pans as compared with other all-metal induction heating systems (normally around 70%) [4], [5].

As shown in Fig. 9, the thermal images of various metallic pans are captured by a thermal scanner (FLUKE TiS 40) after heating for 120 s. It indicates that the average temperatures along the diameter of the iron pan, stainless steel pan, aluminum pan, and copper pan are 105.2 °C, 102.4 °C, 100.3 °C, and 99.5 °C, respectively, at the same operating frequency of 30 kHz. It confirms that all metallic pans can be heated successfully in the proposed induction heating system.

V. Conclusion

In this paper, an all-metal domestic induction heating system has been proposed and implemented. The key is to newly employ double-layer coils and utilize the MRC mechanism to effectively heat both the ferromagnetic and non-ferromagnetic pans at the same operating frequency. Unlike normal MRC for wireless power transfer, the resonant coil (upper coil) not only serves to boost the power transfer from the transmitter (lower coil) to the receiver (pan) but also provides high current to strengthen the magnetic coupling and hence the dissipated power in the non-ferromagnetic pan. The required high current is shifted from the lower primary coil to the upper resonant coil, hence significantly reducing the current stress at the power source. Theoretical analysis, numerical simulation, and experimentation are given to validate the proposed system.

Acknowledgment

The work was supported by the University of Hong Kong, Hong Kong, under Grant 201409176054.

References

[1] Ó. Lucía, P. Maussion, E. J. Dede, and J. M. Burdío, "Induction heating technology and its applications: Past developments, current technology, and future challenges," *IEEE Trans. Ind. Electron.*, vol. 61, no. 5, pp. 2509–2520, May 2014.

[2] T. Lubin, D. Netter, J. Leveque, and A. Rezzoug, "Induction heating of aluminum billets subjected to a strong rotating magnetic field produced by superconducting windings," *IEEE Trans. Magn.*, vol. 45, no. 5, pp. 2118–2127, May 2009.

[3] T. Hirokawa, E. Hiraki, T. Tanaka, M. Okamoto, and M. Nakaoka, "The practical evaluations of time-sharing high-frequency resonant soft-switching inverter for all metal IH cooking appliances," in *Proc. IEEE Annu. Conf. Ind. Electron. Soc.*, Oct. 2012, pp. 3302–3307.

[4] I. Millán'n, J. M. Burdío, J. Acero, O. Lucía, and S. Llorente, "Series resonant inverter with selective harmonic operation applied to all-metal domestic induction heating," *IET Power Electron.*, vol. 4, no. 5, pp. 587–592, May 2011.

[5] H.-P. Park and J.-H. Jung, "Load-adaptive modulation of a series-resonant inverter for all-metal induction heating applications," *IEEE Trans. Ind. Electron.*, vol. 65, no. 9, pp. 6983–6993, Sep. 2018, doi: 10.1109/TIE.2018.2793270.

[6] Z. Zhang, K. T. Chau, C. Qiu, and C. Liu, "Energy encryption for wireless power transfer," *IEEE Trans. Power Electron.*, vol. 30, no. 9, pp. 5237–5246, Sep. 2015.

[7] C. Jiang, K. T. Chau, T. W. Ching, C. Liu, and W. Han, "Time-division multiplexing wireless power transfer for separately excited DC motor drives," *IEEE Trans. Magn.*, vol. 53, no. 11, Nov. 2017, Art. no. 8205405.

[8] C. Jiang, K. T. Chau, Y. Leung, C. Liu, C. H. T. Lee, and W. Han, "Design and analysis of wireless ballastless fluorescent lighting," *IEEE Trans. Ind. Electron*, to be published, doi: 10.1109/TIE.2017.2784345.

[9] W. Han, K. T. Chau, and Z. Zhang, "Flexible induction heating using magnetic resonant coupling," *IEEE Trans. Ind. Electron.*, vol. 64, no. 3, pp. 1982–1992, Mar. 2017.

[10] W. Han, K. T. Chau, Z. Zhang, and C. Jiang, "Single-source multiple-coil homogeneous induction heating," *IEEE Trans. Magn.*, vol. 53, no. 11, Nov. 2017, Art. no. 7207706.

[11] T. Tanaka, "A new induction cooking range for heating any kind of metal vessels," *IEEE Trans. Consum. Electron.*, vol. 35, no. 3, pp. 635–641, Aug. 1989.